Mesoscale Structure of an Oklahoma Squall Line

JUDITH STOKES BRADBERRY[1]

National Severe Storms Laboratory, Norman OK 73069

21 June 1979 and 6 January 1981

ABSTRACT

A squall line, which passed through the National Severe Storms Laboratory mesonetwork in Oklahoma on 26 April 1969, is analyzed to determine the mesoscale structure. The analyses are based on data from 23 rawinsonde ascents, 29 automatically recording surface stations, and radar PPI coverage.

A composite analysis revealed the existence of a mesoscale descent-ascent doublet in the vertical-motion pattern. The descent was centered about 10 km ahead of, and the ascent about 5 km behind the leading edge of the radar echoes. The downdraft appears to be driven by evaporative cooling from the tops of cumulus clouds and cooling due to the dissipation of a middle cloud layer; the updraft seems to be driven mainly by condensational heating. On the basis of this and other cases, it is tentatively concluded that this doublet of mesoscale vertical motions may be a distinguishing feature of large convective storm systems in their mature stages of development, whether they be of frontal or of squall-line character.

1. Introduction

In an earlier paper, Sanders and Paine (1975, hereafter referred to as SP) examined the case of a convectively active cold front which passed through the National Severe Storms Laboratory's (NSSL) mesonetwork in central Oklahoma. The mesonetwork data was analyzed to determine the structure and thermodynamics of this system and the effects of convection on the mean mesoscale atmosphere.

In this note a squall line, which occurred on 26 April 1969, is investigated in a similar manner as the SP study to resolve its mesoscale structure. The line, which formed in the vicinity of a slow-moving cold front in northwestern Oklahoma, strengthened during the day and moved east-southeastward ahead of the front through the mesonetwork.

[1] Present affiliation: National Weather Service Forecast Office, Atlanta, GA 30354. (This work is an extension of the author's M.S. thesis at the Dept. of Meteorology, Massachusetts Institute of Technology, Cambridge 02139.)

2. Organization of data

On 26 April 1969, a portion of a squall line migrated through the NSSL mesonetwork (Fig. 1) between 1500 and 1800 CST. Thus, it was possible to examine the mesoscale structure of the storm system. Observations from 29 recording surface stations, vertical soundings from 23 rawinsonde ascents and Plan Position Indicator (PPI) radar coverage at elevation angles for 0–18° form the basis for this study. Radar coverage was provided by a modified WSR-57 10 cm radar at NSSL Headquarters surface station, 5E.

The system was studied in a reference frame relative to the *L*eading *E*dges of the *R*adar *E*choes

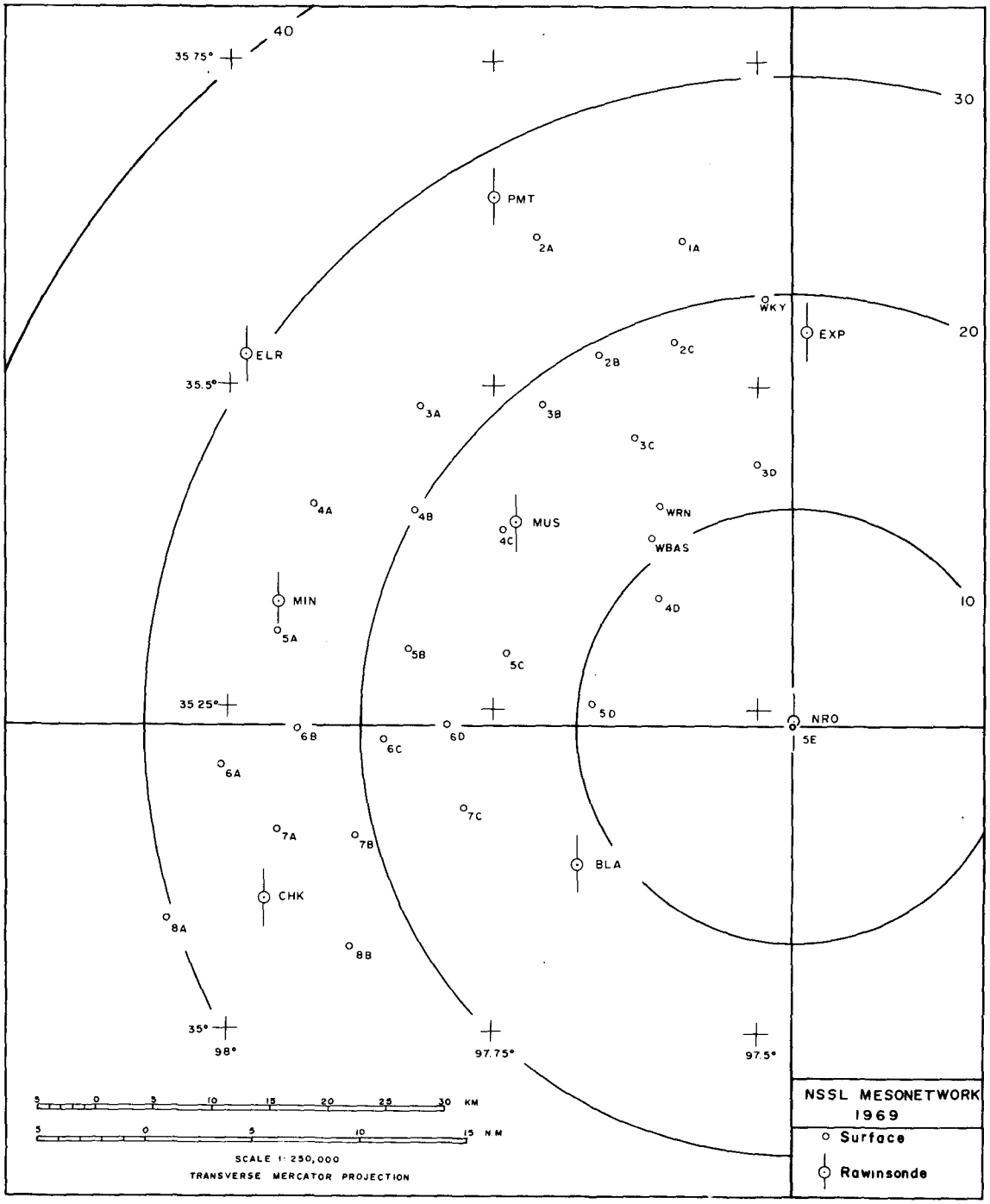

FIG. 1. The 1969 NSSL upper air and surface mesonetwork.

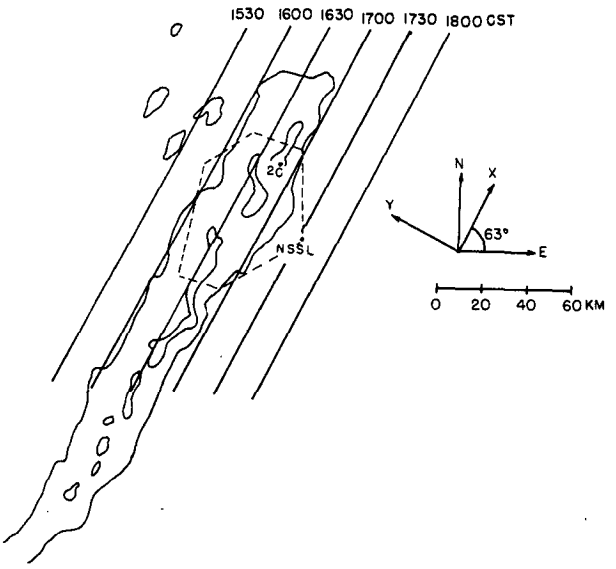

FIG. 2. Isochrones (CST) of the LERE line (see text). Radar PPI presentation at 0° elevation at 1650 CST. Intensity levels 1 and 4 are shown. A coordinate system moving with the line is on the right. Area enclosed by dashed lines is NSSL mesonetwork.

(LERE) because of their linear structure. Here, we define a smoothed average leading edge of the radar echo line, hereafter referred to as LERE, as a straight line moving at a constant speed v of 8.8 m s^{-1} lying usually between the first and second reflectivity contours. The advance of the LERE line through the network and a coordinate system moving with the line is shown in Fig. 2. The y axis passes through station 5E. The time coordinate (t) is defined to be coincident with the y coordinate by the relation $t = y/v$.

With only 23 soundings, the data is too sparse to permit the representation of significant meteorological variables in all three spatial dimensions and in time. But the organization of the storm system into a well-defined line and the short time span of the observational period suggest preparation of a composite analysis of the rawinsonde data based on the assumptions of a steady state and of no variation in the direction parallel to the LERE.[2] Therefore, the variables were analyzed and the results are presented in a vertical plane transverse to the LERE. However, lack of data prohibited the measurement of variations in time, so it is not known whether the assumption of steady state is accurate. Because of strong south-southwesterly flow, the assumption of no variations along the LERE is not valid in budget calculations. Nevertheless the results are still presented in a plane transverse to the LERE, since this presentation makes best use of the data.

Shown in Fig. 3 are rawinsonde paths projected on the y-p plane. Soundings were terminated at 400 mb. To avoid inclusion of small irregularities in the rawinsonde data analysis, 50 mb means of all pertinent meteorological variables are used as suggested by Fankhauser (1969). The mean values are assigned

[2] Precedent for such an approach can be found in the work of Newton (1950, 1963).

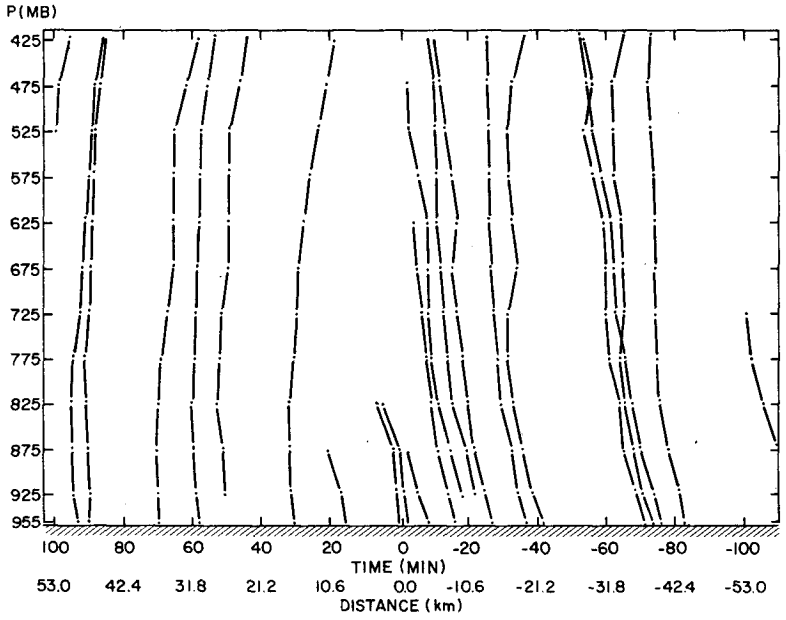

FIG. 3. Rawinsonde paths projected on the $y(t)$-p plane. Dots represent positions of individual balloons at surface and 50 mb intervals. Abscissa is labeled in both time and distance relative to the LERE.

to the mid-pressure of the layer. However, the mean for the lowest layer from the surface to 950 mb represents a thickness of only 9 mb.

Variables were analyzed in x and y over a rectangular area, with x ranging between -20 to $+40$ km and y ranging between -58.3 and $+53.0$ km for each of the 12 pressure layers. As stated above, the data were too sparse to permit detailed analysis in all three spatial dimensions and in time; therefore, variables were averaged in x and the results are presented in a vertical plane transverse to the LERE. Limitations of this two-dimensional presentation are discussed in Section 3, below.

Derivatives in the y and p directions were obtained by use of finite difference methods. The pressure interval is 50 mb, while the interval in the y direction is 10.6 km. Derivatives of any quantity in the x direction were obtained by dividing the rectangular grid in half by a line parallel to the y axis, averaging the quantity in x in each half of the grid for each y, assigning this average value to the midpoint in each half section and then using finite differences over an interval of 30 km.

3. Distributions of meteorological variables

a. Horizontal wind components

Wind components along the x and y axes are denoted by u and v, respectively. The dashed lines in Fig. 4 represent the u component. Note the strong vertical shear. The wind field has a strong south-southwesterly component throughout the whole region except in the lower layers on the left, where the strength decreased somewhat. This strong south-southwesterly flow is a reason why the two-dimensional display in the y-p plane presented here cannot fully describe this three-dimensional system.

The v component (relative to the moving frame of reference) is presented as the solid lines in Fig. 4. Strong convergence is noticeable from 0 to +40 min between 900 and 750 mb and between 550 and 450 mb.

b. Vertical wind component

The kinematic method of computing vertical velocities consists of computing the divergence D directly from the observed winds. After the divergence was computed, stepwise integration of the continuity equation

$$\frac{\partial \omega}{\partial p} + D_k = 0 \tag{1}$$

yielded the vertical component of velocity ω at the top of all K layers:

$$\omega(x, y, p_k - \tfrac{1}{2}\Delta p) = \omega(x, y, p_{sfc}) + \sum_{1}^{K} D_K \Delta_p, \tag{2}$$

where $\Delta p = 9$ mb for $K = 1$ and 50 mb for all other K and $\omega(x,y,p_{sfc})$ is assumed to be zero; D_K is the mean divergence in the Kth layer assigned to the middle of the layer at pressure level p_K.

The vertical motion pattern presented in Fig. 5 was calculated from (2) at the top of all K layers and then averaged in x. The most prominent feature is the descent-ascent doublet between -50 and $+60$

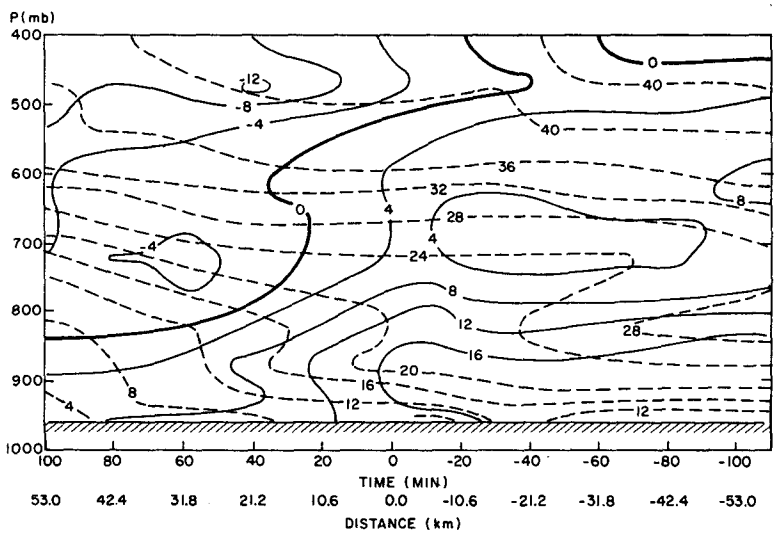

FIG. 4. Dashed lines represent u component of wind (m s^{-1}) with respect to a fixed coordinate system. Positive values for air moving into the page. Solid lines represent v component of wind (m s^{-1}) with respect to the moving coordinate system. Positive values for air moving toward the left. The squall line is oriented along the x axis; the positive x direction is into the page.

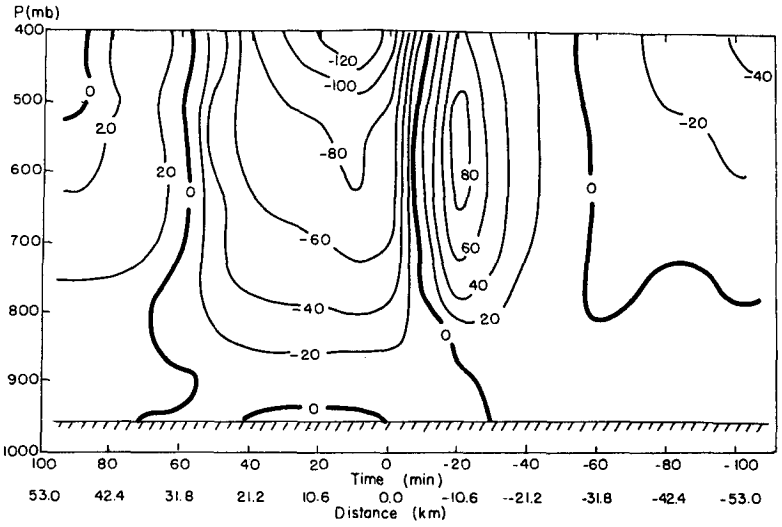

FIG. 5. Mesoscale vertical motions (10^{-3} mb s^{-1}).

min, the descent being centered at −20 min and the ascent centered at +10 min. SP also found a similar doublet pattern in their examination of the frontal disturbance. Fankhauser's (1974) vertical motions, obtained in his analysis of a squall-line case, also showed a descent-ascent doublet.

c. *Potential temperature and mixing ratio*

The potential temperature field appears in Fig. 6. In the lower layers up to 850 mb before −20 min, the potential temperature distribution is nearly horizontal. After −20 min between 750 and 550 mb the analysis shows a general cooling trend.

An analysis of the mixing ratio following the procedure discussed in Section 2 indicates relative humidities ~50–60% in the location of most intense and persistent radar echoes. This inconsistency is attributable to lack of soundings in this region, where the air must be saturated or very nearly so. The analysis was adjusted in this region to be consistent with the radar echoes by accepting the temperature analysis as correct and by changing the mixing ratio values so that the relative humidity in this region was 94%. This somewhat arbitrary value corresponds to the average value of relative humidity over all the 29 recording surface stations. The value was taken as a lower limit of what might be expected aloft.

The resulting field of mixing ratio q is shown in Fig. 7. Because of the above adjustments, the strength of the horizontal gradients near −20 and near +45 min may be excessive. The tight vertical

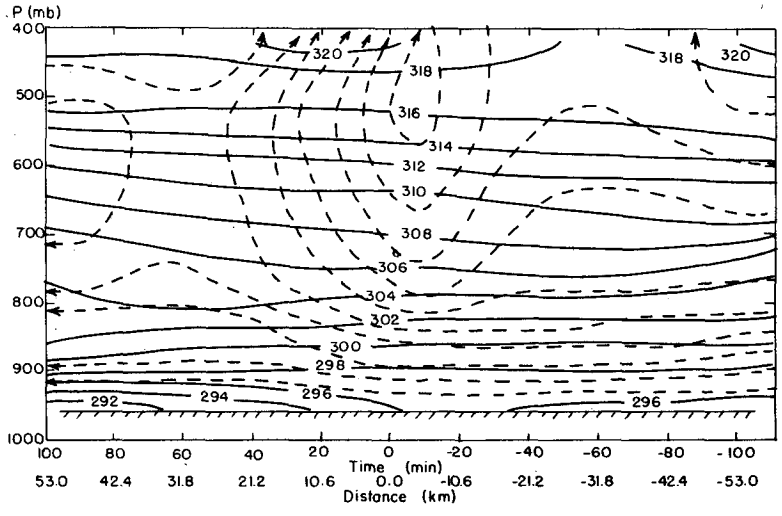

FIG. 6. Mesoscale potential temperature $\theta(K)$. Dashed lines are streamfunction lines of flow relative to the LERE line at intervals of 400 mb m s^{-1}.

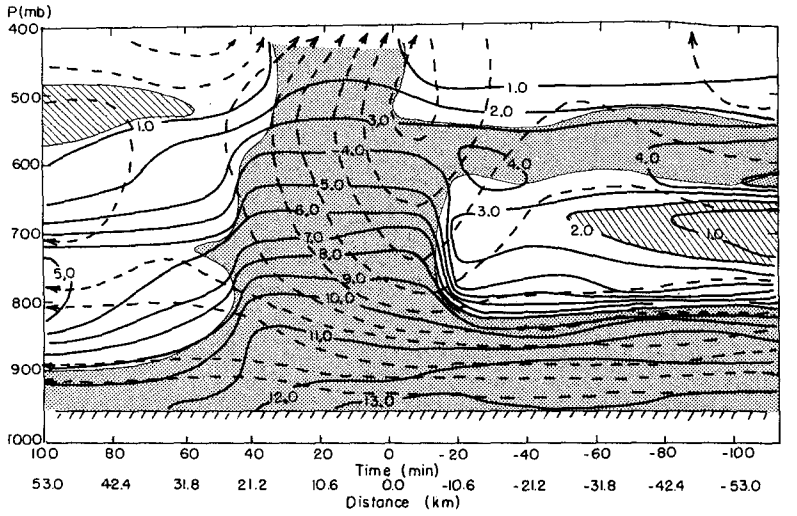

FIG. 7. Mesoscale mixing ratio q (g kg^{-1}). Streamfunction lines are as in Fig. 6. Hatching and stippling represent, respectively, areas of relative humidity less than 25% and greater than 75%.

gradient before −20 min in the 850–750 mb layer is supported by individual soundings, especially those launched in the southwestern part of the network prior to the arrival of the LERE, which show a moist layer from the surface up to ~800 mb abruptly capped by a dry layer which extended up to ~600 mb with another moist layer aloft. Examination of individual soundings and surface observations indicates that the upper moist layer prior to −20 min represents a cloud deck of altocumulus mainly in the southwestern part of the network.

4. Mesoscale budgets

a. Discussion of concepts

The effects of convection on the heat and moisture structure of the mean mesoscale atmosphere can be estimated as residuals in budgets in which the transports by the mesoscale motions are calculated. As in the SP study, the problem is approached by considering the budget for a quantity Q in a mesoscale volume 50 mb deep, 10.6 km in the y direction, and 30 km in the x direction. The overbar is used to indicate an average over such a volume and the prime is used to indicate deviations from this average value. The meteorological variables which appeared in the previous section are synonymous with the corresponding barred quantities presented in this section. We have

$$\bar{\dot{Q}} = \frac{\partial \bar{Q}}{\partial t} + \frac{\partial}{\partial x}(\bar{u}\bar{Q}) + \frac{\partial}{\partial y}(\bar{v}\bar{Q}) + \frac{\partial}{\partial p}(\bar{\omega}\bar{Q}) + \frac{\partial}{\partial x}(\overline{u'Q'}) + \frac{\partial}{\partial y}(\overline{v'Q'}) + \frac{\partial}{\partial p}(\overline{\omega'Q'}), \quad (3)$$

where $\bar{\dot{Q}}$ is the real source. The apparent source is denoted by

$$\dot{Q}^* = \frac{\partial \bar{Q}}{\partial t} + \frac{\partial}{\partial x}(\bar{u}\bar{Q}) + \frac{\partial}{\partial y}(\bar{v}\bar{Q}) + \frac{\partial}{\partial p}(\bar{\omega}\bar{Q}), \quad (4)$$

the rate of change following the mesoscale motion. If we assume that horizontal eddy fluxes are much smaller than the vertical fluxes, we drop horizontal flux terms and denote a virtual source by

$$\dot{Q}^v = -\frac{\partial}{\partial p}(\overline{\omega'Q'}). \quad (5)$$

This is assumed to essentially represent the effects of convective elements, except in the surface boundary layer where the effects of surface friction are included. Rewriting (3) using (4) and (5)

$$\dot{Q}^* = \bar{\dot{Q}} + \dot{Q}^v.$$

From the analysis of the mesoscale mean fields all of the terms of $\dot{Q}^*$ can be calculated except for $\partial\bar{Q}/\partial t$. We shall denote $\dot{Q}^* - \partial\bar{Q}/\partial t$ as Q^{**} and refer to it as the approximate source. This notation differs from that of SP. Since they were able to determine $\partial\bar{Q}/\partial t$ the entire apparent source, $\dot{Q}^*$, was computed. In this case $\partial\bar{Q}/\partial t$ as well as the virtual source $\dot{Q}^v$ can be determined only as residuals.

b. Potential temperature

The approximate apparent source of $\bar{\theta}$ is shown in Fig. 8. Apparent heating and cooling are primarily taking place in regions of mesoscale ascent and descent, respectively. Before −10 min in the layer between 850 and 750 mb there is an apparent sink of

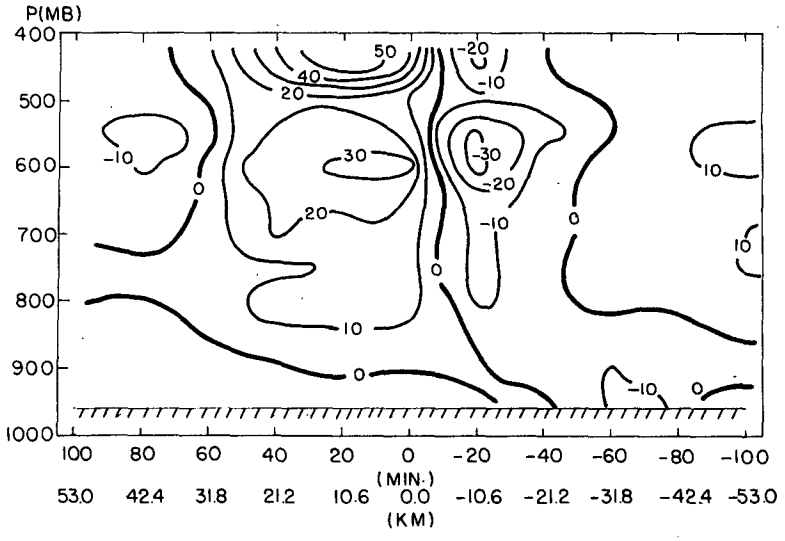

FIG. 8. Approximate apparent source of potential temperature $\dot{\theta}^{**}$ labeled in units of 10^{-2} K min^{-1}.

$\bar{\theta}$. It is believed to be in this region that the initial cumulus convective clouds, triggered by low-level convergence, were evaporating into the dry air above 800 mb. Above 650 mb the cooling is probably due to evaporation of the middle cloud deck entering the southwestern part of the network. These regions of cooling appear to be driving the mesoscale subsidence.

c. *Mixing ratio*

The approximate apparent source of $\bar{q}$ is presented in Fig. 9. The source at −20 min centered near 800 mb is apparently due to evaporation into the dry air in middle levels of cumulus convective clouds, which initially resulted from low-level convergence. The strength of this source may be somewhat exaggerated, because of reasons mentioned previously. It is accompanied by a much weaker sink below. The source above 600 mb near −20 min may be due to evaporation of the cloud deck entering the southwestern part of the network.

The loss of $\bar{q}$ in the region of mesoscale ascent between 0 and +60 min is due primarily to condensation. Rain at the surface relative to the LERE coincides with the mesoscale ascent region. The maximum rainfall rate occurs at +20 min (some 10 min after peak ascent is reached in this region). The

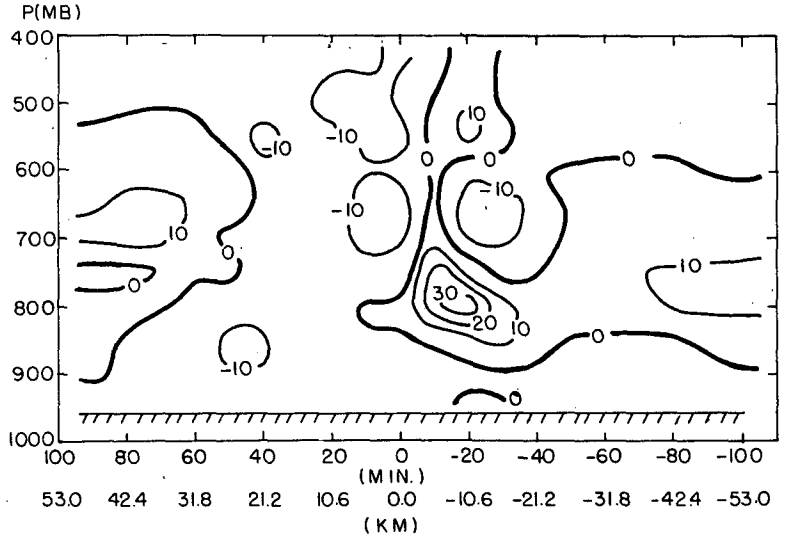

FIG. 9. Approximate apparent source of mixing ratio $\dot{q}^{**}$ labeled in units of 10^{-2} g kg^{-1} min^{-1}.

apparent loss between 700 and 600 mb just prior to −20 min is not readily explained.

5. Concluding remarks

This study has examined the 26 April 1969 squall line which moved ahead of a surface cold front through the NSSL mesonetwork. Although the analysis of the squall-line system was presented in a two-dimensional display transverse to the leading edge of the radar echoes to permit maximum use of the available data, the three-dimensional characteristics of the system were evident in the rawinsonde observations.

Despite the three-dimensional structure of the system, the two-dimensional display gave some interesting results. Surface convergence of the order of 10^{-3} s^{-1} triggers new convective activity. An intense mesoscale descent-ascent doublet develops, the descent being centered ~10 km ahead of the leading edge of the radar echoes and the ascent centered ~5 km behind it. Peak speeds in the descending branch reach ~1.3 m s^{-1} at 550 mb, while peak speeds in the zone of ascent reach ~2.5 m s^{-1} at 400 mb. These vertical currents appear to be driven by a corresponding doublet of cooling and heating with peak rates of 0.3 K min^{-1} of cooling and 0.5 K min^{-1} of heating. The cooling is produced by evaporation within superimposed convection.

This descent-ascent doublet was also characteristic of cases studied by Fankhauser (1974) and Sanders and Paine (1975). The synoptic situation was not the same in all three cases. Two cases were squall lines, while the convection resulted from frontal overrunning in the other. It appears that the mesoscale vertical motion doublet may be a distinguishing feature of large convective storm systems whether they be of frontal or of squall line character.

The lack of data prevented the complete analysis of the effects of convective activity on the mean mesoscale atmosphere. Future studies of this kind will require more soundings, both in and out of storm areas. Although Barnes (1974)[3] suggests no economically feasible combination of rawinsondes will ever completely resolve flow patterns and thermodynamic structure within severe storms, rawinsondes are still the most reliable system for providing wind data at many vertical levels in the immediate storm environment.

Acknowledgments. I am grateful to Prof. Frederick Sanders, MIT, for introducing me to this case and his helpful assistance throughout this research work. The useful comments of Drs. Robert Davies-Jones and Peter Ray of NSSL and Dr. Robert Wilhelmson of University of Illinois are acknowledged. I also acknowledge Ms. Sandra Mudd for her help in preparing the manuscript.

REFERENCES

Barnes, S. L., 1974: Papers on Oklahoma thunderstorms, April 29–30, 1970. NOAA Tech. Memo. ERL NSSL-69. [NTIS COM-74-11474/AS].

Fankhauser, J. C., 1969: Convective processes resolved by a mesoscale rawinsonde network. *J. Appl. Meteor.*, **8**, 778–798.

——, 1974: The derivation of consistent fields of wind and geopotential height from rawinsonde data. *J. Appl. Meteor.*, **13**, 637–646.

Newton, C. W., 1950: Structure and mechanism of the prefrontal squall line. *J. Meteor.*, **7**, 210–222.

——, 1963: Dynamics of severe convective storms. *Severe Local Storms, Meteor. Monogr.*, No. 27, Amer. Meteor. Soc., 33–58.

Sanders, F., and R. J. Paine, 1975: The structure and thermodynamics of an intense mesoscale convective storm in Oklahoma. *J. Atmos. Sci.*, **32**, 1563–1579.